http://dx.doi.org/10.21577/0100-4042.20170871 *Quim. Nova,* Vol. 45, No. 6, 742-749, 2022

Educação

RING CURRENT IN ANTHRACENE AND PHENANTHRENE: CORRECTION TO HÜCKEL PARAMETERS

Yuanita P. D. Sudarso[a], Arifin L. Maulana[b], Agoes Soehiani[a], and Inge M. Sutjahja[a,*]
[a]Department of Physics, Faculty of Mathematics and Natural Sciences, Institut Teknologi Bandung, Bandung, Indonesia
[b]Department of Physics Engineering, Faculty of Industrial Technology, Institut Teknologi Bandung, Bandung, Indonesia

Recebido em 23/09/2021; aceito em 16/12/2021; publicado na web em 10/03/2022

Excessive degeneracy in the ground state of the π-electron energy levels of anthracene was removed using the Hückel method by correcting the Coulomb integral of the four central carbon atoms. A further correction to the resonance integral was proposed based on the ring-current model, which describes the π-ring current flow along the molecule's perimeter, by introducing a new parameter for the bridge carbon atoms expressed as a fraction of the resonance energy. The solution to the Hamiltonian was obtained based on the symmetry group theory, which provides the advantage of solving the determinant matrix or secular equations in a particular irreducible representation with a relatively small matrix dimension. The results were further analyzed to determine the bond order and bond length. The values of the harmonic oscillator model of aromaticity, GEO, and EN indices of aromaticity and their ratio for the central and outer rings of benzene were used to evaluate the validity of the correction. Applying the same method to phenanthrene as a topological analog of anthracene allows for an interesting comparison of the stabilities of the two molecules.

Keywords: Hückel methods; anthracene; phenanthrene; ring current model; harmonic oscillator model of aromaticity.

INTRODUCTION

The Hückel molecular orbital (HMO) theory is the simplest theory for investigating the ground state of a conjugated organic molecule with a planar conformation that has a π-electron system (See Ref. 1 for a complete review). Despite the roughness of its approximations, the validity of this model is undisputable. The HMO theory is indispensable as it provides a basis for understanding conjugated hydrocarbons.[2] HMO is related to Hückel's aromaticity $(4n + 2)$-rule, which indicates that cyclic conjugated hydrocarbons with $(4n + 2)\pi$-electrons are aromatic, while those with $(4n)\pi$-electrons are antiaromatic.[1] In many cases, a molecule's aromaticity is related to increased stability, small bond length alternation, and unique magnetic properties associated with the ring current.[3] However, the excessive degeneracy in the energy levels obtained from Hückel theory is often due to a Hamiltonian symmetry, which is higher than that of the molecule,[4] and a simplified Hamiltonian, which ignores all non-nearby-neighbor interactions.[5]

In the case of benzene (C_6H_6), the Hückel theory predicts a homogeneous bond order of all nearby neighbor carbon atoms, suggesting a resonance stabilization of benzene.[1,6,7] In this case, the energy level of benzene has two doubly degenerate states (Figure 1(a)) that are related to the high symmetry (point group D_{6h}) of the molecule.[1,6,7] In the case of naphthalene ($C_{10}H_{10}$) with two-fused benzene rings, lowering the symmetry of the molecule (point group D_{2h}) gives rise to non-degenerate energy levels (Figure 1(b)).[6,7,8] Unexpected degeneracy also occurs in anthracene ($C_{14}H_{10}$), as shown in Figure 1(c), consisting of 3 fused benzenes that belong to the same point group as naphthalene.[8] From a theoretical point of view, non-degenerated energy levels were predicted from the irreducible representation of D_{2h}, as confirmed from the semi-empirical self-consistent field (SCF) calculation.[9]

An old-fashioned paradigm of aromaticity states that aromatic molecules support diatropic ring currents, whereas antiaromatic molecules support paratropic ring currents in the presence of an external magnetic field.[10] Delocalization of the π-electron develop into the assignment of aromaticity as a visual inspection of a map of induced (π) current density, the so-called ring current model (RCM).[11] Hence, an external magnetic field applied perpendicular to the ring produces a ring current that induces a counter field. Delocalization of the π-electrons of the molecule affects the long-range contributions of the induced magnetic field. On the other hand, since the σ-electrons are more localized than π-electrons, they generate a short-range magnetic response with diatropic areas along with the bonds and a paratropic response in the molecular center.[12] Application of the RCM to benzene, naphthalene, and anthracene shows that those molecules sustain π-ring currents over all the carbon skeleton beyond the molecular periphery.[11,13-16] Recently, the existence of circular currents in the macroscopic ring structures of benzene, naphthalene, and anthracene has been emulated experimentally by a network of macroscopic microwave resonators.[17]

In this study, a correction to the Hückel theory was applied to anthracene by assigning a different Coulomb integral parameter to the four central carbon atoms because of their particular environment,[18] and different resonance integrals based on a phenomenological description of the π-ring current in a magnetic field normal to the molecular plane.[11,14,15] Because of the high symmetry of the molecule, the solution to the Schrödinger equation will be obtained by employing the group theory. The resulting linear combination coefficients of the molecular orbitals were used to calculate the bond order and bond length. The validity of the results was examined using the harmonic oscillator model of aromaticity (HOMA) index,[3,19-21] which is widely accepted for measuring aromaticity based on the structure of the molecule.[22] Compared to the magnetic-based nucleus-independent chemical shift (NICS) index reported by Schleyer *et al.*[23] and the electronically based para-delocalization index (PDI),[24] the HOMA is much simpler, more successful, and more widely used.[19,25] We also applied the same method to phenanthrene, a topological analog of anthracene, albeit with different ring currents. Hence, theoretical calculations show that for anthracene, the ring currents are mainly localized on the central benzene ring, whereas for phenanthrene, they are more intense in the outer benzene ring.[16,26] We compared the stability of these two molecules based on the molecular orbital energy diagram. The calculation was performed using MATLAB®

*e-mail: im_sutjahja@itb.ac.id

software to solve the reduced Hamiltonian based on an irreducible representation (IR) and visualized using Gnuplot©. The results were then compared to those of previous advanced quantum mechanics calculations and experimental studies.

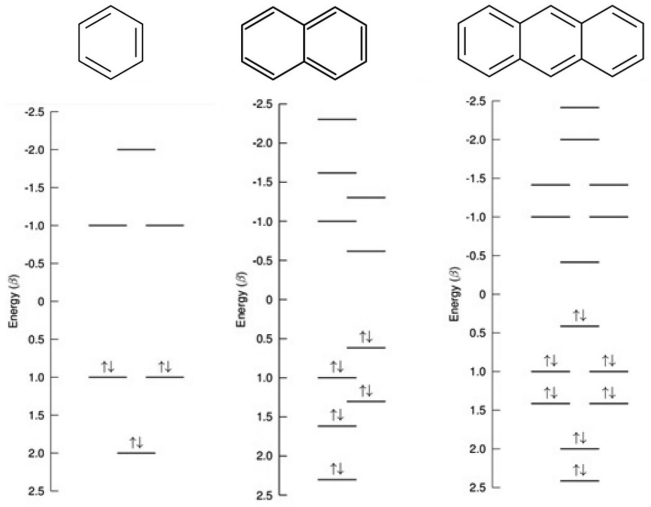

Figure 1. *Molecular structure and the resulting energy level of (a) benzene, (b) naphthalene, and (c) anthracene from Hückel theory*

Hückel molecular orbital theory

The Hückel molecular orbital theory uses a linear combination of the atomic orbital (LCAO) method to solve the Hamiltonian of the π-electron system[1]

$$\hat{H}\psi = E\psi \tag{1}$$

with

$$\psi_n = \sum_{i=1}^{n} c_{n,i} p_i \tag{2}$$

where $c_{n,i}$ is the coefficient of linear combination, and p_i is the $2p_z$ atomic orbital of *the* i^{th} order of the C atom, and n is the total number of carbon atoms that form the molecule. In the Hückel method, the Hamiltonian matrix element is approximated as follows:

(i) All the diagonal elements of the Hamiltonian matrix are assumed to have the same value, namely, the Coulomb integral (α),

$$H_{ij} = \alpha\ ,\ i = j \tag{3}$$

(ii) The nearest neighbor is taken as the resonance integral (β):

$$H_{ij} = \beta\ ,\ i - j = \pm 1 \tag{4}$$

In addition, the overlap integral is diagonal,

$$S_{ij} = \delta_{ij} \tag{5}$$

The resulting coefficient of linear combination can be further used to calculate the bond order, as defined by

$$\rho_{ij} = \nu_n \sum_n c_{ni} c_{nj} \tag{6}$$

where ν_n is the occupation number of π electrons in a particular orbital of the molecule.

The delocalization energy of a molecule is the difference between the total energy of the π electron system and the simple isolated system,

$$E_{deloc} = E_{total,\pi} - E_{isolated} \tag{7}$$

For anthracene and phenanthrene, the isolated system consists of 7 ethylene molecules, and the total energy of one ethylene molecule is 2(α + β). In addition, the HOMO–LUMO energy gap is defined as:

$$E_{gap} = E_{\text{LUMO}} - E_{\text{HOMO}} \tag{8}$$

where E_{LUMO} and E_{HOMO} are the energy of the lowest unoccupied molecular orbital (LUMO) and highest occupied molecular orbital (HOMO), respectively.

Symmetry group theory of anthracene and phenanthrene

The anthracene molecule is shown in Figure 2, along with the numbering of carbon atoms. Each carbon atom donates one p_z atomic orbital as the basis for forming a molecular orbital.

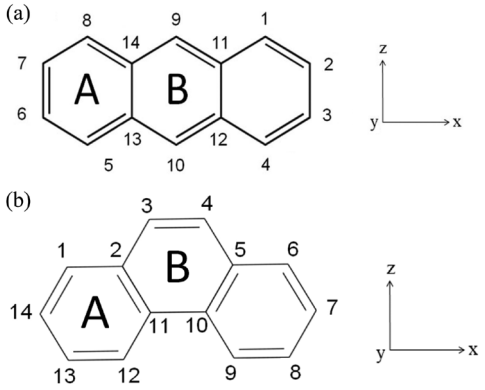

Figure 2. *C-atom numbering of Anthracene (a) and Phenanthrene (b)*

The symmetry group of the anthracene is D_{2h}[8] with a character table shown in Table 1.[7] This group contains eight elements: the identity element (I), three rotations through angle π about the coordinate axes (C_{2z}, C_{2y}, C_{2x}), the inversion (i), and three reflections (σ_{xy}, σ_{xz}, σ_{yz}). As we see in Table 1, all the irreducible representations of D_{2h} are one-dimensional; hence, no degeneracy should be expected.

Table 1. Character table for D_{2h} point group

D_{2h}	I	C_{2z}	C_{2y}	C_{2x}	i	σ_{xy}	σ_{xz}	σ_{yz}
A_g	1	1	1	1	1	1	1	1
B_{1g}	1	1	−1	−1	1	1	−1	−1
B_{2g}	1	−1	1	−1	1	−1	1	−1
B_{3g}	1	−1	−1	1	1	−1	−1	1
A_u	1	1	1	1	−1	−1	−1	−1
B_{1u}	1	1	−1	−1	−1	−1	1	1
B_{2u}	1	−1	1	−1	−1	1	−1	1
B_{3u}	1	−1	−1	1	−1	1	1	−1

On the other hand, the symmetry group of the phenanthrene is C_{2v}[8], which contains four elements: the identity element (I), rotation through angle π about z the coordinate axes, and two vertical plane reflections (σ_{xz}, σ_{yz}). The corresponding character tables are listed in Table 2.[7,27]

Table 2. Character table for C_{2v} point group

C_{2v}	I	C_2	$\sigma_v(xz)$	$\sigma_v(yz)$
A_1	1	1	1	1
A_2	1	1	−1	−1
B_1	1	−1	1	−1
B_2	1	−1	−1	1

When a symmetry transformation R is applied to the orbital (Figure 2), we obtain

$$R \rightarrow p_z(i) = \sum_j \Gamma(R)_{ij} p_z(j) \quad (9)$$

where $\Gamma(R)_{ij}$ is the ij element of the matrix that represents the symmetry element R. Under these symmetry operations, the 14-p_z orbital transforms accordingly. The characteristics of this matrix of anthracene are:

D_{2h}	I	C_{2z}	C_{2y}	C_{2x}	i	σ_{xy}	σ_{xz}	σ_{yz}
Γ	14	0	-2	0	0	-14	0	2

while the corresponding characteristics of phenanthrene are:

C_{2v}	I	C_2	$\sigma_v(xz)$	$\sigma_v(yz)$
Γ	14	0	14	0

Symmetry adapted linear combinations (SALCs) are formed using the projection operator,[6,7,27]

$$P^{\mu} = \sum_R \chi^{\mu}(R) * O_R \quad (10)$$

The results of normalized SALCs for anthracene are shown in Table 3. These imply a reduction of a 14×14 Hamiltonian matrix according to the IR representation of D_{2h}, with doubly 3×3 matrices for B_{2g} and A_u IRs, and doubly 4×4 matrices for B_{3g} and B_{1u} IRs. We note that for this particular molecule, there is no SALC for A_g, B_{1g}, B_{2u}, and B_{3u} IRs.

Table 3. The resulted SALC of anthracene (p refers to p_z-orbital)

IR	SALC	IR	SALC
B_{2g}	$\pi_1 = \frac{1}{2}(p_1 + p_4 - p_5 - p_8)$	A_u	$\pi_1 = \frac{1}{2}(p_1 + p_5 - p_4 - p_8)$
	$\pi_2 = \frac{1}{2}(p_2 + p_3 - p_6 - p_7)$		$\pi_2 = \frac{1}{2}(p_2 - p_3 + p_6 - p_7)$
	$\pi_3 = \frac{1}{2}(p_{11} + p_{12} - p_{13} - p_{14})$		$\pi_3 = \frac{1}{2}(p_{11} - p_{12} + p_{13} - p_{14})$
B_{3g}	$\pi_1 = \frac{1}{2}(p_1 - p_4 - p_5 + p_8)$	B_{1u}	$\pi_1 = \frac{1}{2}(p_1 + p_4 + p_5 + p_8)$
	$\pi_2 = \frac{1}{2}(p_2 - p_3 - p_6 + p_7)$		$\pi_2 = \frac{1}{2}(p_2 + p_3 + p_6 + p_7)$
	$\pi_3 = \frac{1}{\sqrt{2}}(p_9 - p_{10})$		$\pi_3 = \frac{1}{\sqrt{2}}(p_9 + p_{10})$
	$\pi_4 = \frac{1}{2}(p_{11} - p_{12} - p_{13} + p_{14})$		$\pi_4 = \frac{1}{2}(p_{11} + p_{12} + p_{13} + p_{14})$

The representation in Table 2 can be reduced into the irreducible ones, namely

$$\Gamma = 3B_{2g} + 4B_{3g} + 3A_u + 4B_{1u}$$

The corresponding IRs and SALCs for phenanthrene are shown in Table 4.

Table 4. The resulted SALC of phenanthrene (p refers to p_z-orbital)

IR	*SALC*	
A_1	$\pi_1 = \frac{1}{\sqrt{2}}(p_1 + p_6)$	$\pi_5 = \frac{1}{\sqrt{2}}(p_8 + p_{13})$
	$\pi_2 = \frac{1}{\sqrt{2}}(p_2 + p_5)$	$\pi_6 = \frac{1}{\sqrt{2}}(p_9 + p_{12})$
	$\pi_3 = \frac{1}{\sqrt{2}}(p_3 + p_4)$	$\pi_7 = \frac{1}{\sqrt{2}}(p_{10} + p_{11})$
	$\pi_4 = \frac{1}{\sqrt{2}}(p_7 + p_{14})$	
B_1	$\pi_1 = \frac{1}{\sqrt{2}}(p_1 - p_6)$	$\pi_5 = \frac{1}{\sqrt{2}}(p_8 - p_{13})$
	$\pi_2 = \frac{1}{\sqrt{2}}(p_2 - p_5)$	$\pi_6 = \frac{1}{\sqrt{2}}(p_9 - p_{12})$
	$\pi_3 = \frac{1}{\sqrt{2}}(p_3 - p_4)$	$\pi_7 = \frac{1}{\sqrt{2}}(p_{10} - p_{11})$
	$\pi_4 = \frac{1}{\sqrt{2}}(p_7 - p_{14})$	

The information shown above justify the reduction of a 14×14 Hamiltonian matrix to become a doubly 7×7 matrix for A_1 and B_1 IRs, according to

$$\Gamma = 7A_1 + 7B_1$$

Bond order and bond length correlation

Pritchard and Sumner[18] introduced a formula for bond length as a function of bond order for benzene, naphthalene, and anthracene as

$$R = s - \frac{s - d}{1 + k\left(\frac{1 - \rho_{ij}}{\rho_{ij}}\right)} \quad (11)$$

where s = 1.54 Å and d = 1.33 Å are the lengths of single and double bonds between sp^2 carbon centers, respectively, and k = 0.765 is a parameter that accounts for the larger force constant of the double bond.[28]

Ring current model

The delocalized property of π-electrons determines the magnetic properties of the molecule. As illustrated in Figure 3, an external magnetic field ($\vec{B}_{ext}$) perpendicular to the ring's molecule produces a ring current for aromatic molecules. According to Biot–Savart's law, this ring current induces a counter magnetic field, ($\vec{B}_{ind}$) , with a circular orientation across the molecule's plane.[12-13]

Inside the molecule, $\vec{B}_{ext}$ is in the opposite direction as $\vec{B}_{ind}$, while outside of the molecule $\vec{B}_{ext}$ is in the same direction as $\vec{B}_{ind}$. Thus, the total magnetic field outside the ring is more significant than that inside the ring. For antiaromatic molecules, the reverse situation occurs. Hence, aromaticity is commonly associated with a diamagnetic ring current or diatropic ring current, whereas antiaromaticity is associated with a paratropic ring current.

Both diatropic and paratropic currents are experimentally detectable by their contribution to chemical shifts. Theoretically, the assignment of aromaticity is investigated by visualizing the induced π-current density map through perturbation theory.[10-15] The results for polycyclic aromatic hydrocarbon (PAH) molecules such as benzene, naphthalene, and anthracene show the flow of π-ring currents over

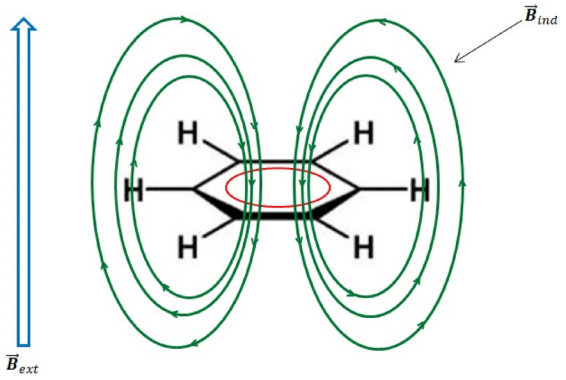

Figure 3. *Illustration of the ring current model of an aromatic molecule*

the molecular perimeter, with weak diamagnetic π-vortices around the center of each ring and the midpoint of the C–C bond connecting them.[11,13-14] This result agrees with the circuit model proposed by Pauling[29] to account for the diamagnetic anisotropy of some aromatic molecules.

Harmonic oscillator model of aromaticity (HOMA)

Aromaticity has been the central concept in organic chemistry for a long time.[19] One measure of aromaticity is structurally based-HOMA[3,19] that was originally defined as

$$\text{HOMA} = 1 - \frac{\alpha}{n}\sum_i \left(R_{opt} - R_i\right)^2 \tag{12}$$

where R_i is the i^{th} bond length in the analyzed molecule's ring, n is the number of C–C bonds in the ring of the molecule, and α is a normalization factor making the unitless HOMA index equal to 1 for perfectly aromatic benzene and 0 for a perfectly alternating hypothetical Kekulé cyclohexatriene ring. Optimal bond length, R_{opt}, is the proper bond length for fully aromatic molecules and denotes the bond length for which expansion to the single bond and compression to the double bond requires the same energy.[3] For carbocyclic molecules, the HOMA index defined in Eq. (12) can also be expressed as:[3,20,21]

$$\text{HOMA} = 1 - \text{GEO} - \text{EN} \tag{13a}$$

with

$$\text{GEO} = \frac{\alpha}{n}\sum_i \left(R_i - R_{av}\right)^2 \tag{13b}$$

$$\text{EN} = \alpha\left(R_{av} - R_{opt}\right)^2 \tag{13c}$$

and

$$R_{av} = \frac{1}{n}\sum_i R_i \tag{14}$$

where R_{av} is the average bond length for a ring of the molecule. Thus, two contributions to the HOMA index have been considered to mean the decrease in aromaticity of the π-electron system arising from independent mechanisms, i.e., (i) GEO as the degree of bond length alternation; and (ii) EN as the extension of the bonds over the mean bond length.[3,20,21] For the C-C bond, using 1,3 butadiene as a reference (with R_s = 1.467 Å and R_d = 1.349 Å as reference bond lengths) one can obtain R_{opt} = 1.388 Å and α = 257.7 Å^{-2}.[3,20,21]

Correction to Hückel parameters

Correction to the Hückel method was performed because the carbon atoms at positions 11, 12, 13, 14 for anthracene have a different environment compared to those at other positions, and they are more electronegative compared to the others.[18] Similarly, for phenanthrene, correction was performed for the carbons at positions 2, 5, 10, and 11. In addition, the π-ring current in anthracene and phenanthrene describes the π-current flow through the perimeter of the molecule.[11,14,15,16,26] Two parameters were proposed to describe the change in the Coulomb energy of C11, C12, C13, and C14 of anthracene and C2, C5, C10, and C11 of phenanthrene:

$$\alpha' = \alpha + a\,|\beta| \tag{15}$$

as well as the resonance energy between C11–C12 and C13–C14 of anthracene and C2–C11 and C5–C10 of phenanthrene, as

$$\beta' = \gamma\,|\beta| \tag{16}$$

In this case, for anthracene, the secular determinant equations for each irreducible representation of the Hückel matrix become:

$$B_{2g}: \quad H = \begin{vmatrix} \alpha - E & \beta & \beta \\ \beta & \alpha + \beta - E & 0 \\ \beta & 0 & \alpha' + \beta' - E \end{vmatrix} = 0$$

$$A_u: \quad H = \begin{vmatrix} \alpha - E & \beta & \beta \\ \beta & \alpha - \beta - E & 0 \\ \beta & 0 & \alpha' - \beta' - E \end{vmatrix} = 0$$

$$B_{3g}: \quad H = \begin{vmatrix} \alpha - E & \beta & 0 & \beta \\ \beta & \alpha - \beta - E & 0 & 0 \\ 0 & 0 & \alpha - E & \sqrt{2}\beta \\ \beta & 0 & \sqrt{2}\beta & \alpha' - \beta' - E \end{vmatrix} = 0$$

$$B_{1u}: \quad H = \begin{vmatrix} \alpha - E & \beta & 0 & \beta \\ \beta & \alpha + \beta - E & 0 & 0 \\ 0 & 0 & \alpha - E & \sqrt{2}\beta \\ \beta & 0 & \sqrt{2}\beta & \alpha' + \beta' - E \end{vmatrix} = 0$$

while for phenanthrene they become:

$$A_1 : H = \begin{vmatrix} \alpha & \beta & 0 & \beta & 0 & 0 & 0 \\ \beta & \alpha' & \beta & 0 & 0 & 0 & \beta' \\ 0 & \beta & \alpha + \beta & 0 & 0 & 0 & 0 \\ \beta & 0 & 0 & \alpha & \beta & 0 & 0 \\ 0 & 0 & 0 & \beta & 0 & \beta & 0 \\ 0 & 0 & 0 & 0 & \beta & \alpha & \beta \\ 0 & \beta' & 0 & 0 & 0 & \beta & \alpha' + \beta' \end{vmatrix} = 0$$

$$B_1 : H = \begin{vmatrix} \alpha & \beta & 0 & -\beta & 0 & 0 & 0 \\ \beta & \alpha' & \beta & 0 & 0 & 0 & -\beta' \\ 0 & \beta & \alpha - \beta & 0 & 0 & 0 & 0 \\ -\beta & 0 & 0 & \alpha & \beta & 0 & 0 \\ 0 & 0 & 0 & \beta & 0 & \beta & 0 \\ 0 & 0 & 0 & 0 & \beta & \alpha & \beta \\ 0 & -\beta' & 0 & 0 & 0 & \beta & \alpha' - \beta' \end{vmatrix} = 0$$

The values of a and γ were varied within the range $0 < a < 1.0$ and $0.1 < \gamma < 1.6$, respectively. We note that a set value of $a = 0$ and $\gamma = 1$ refers to the original Hückel parameter.

The bond length was calculated based on Eq. (11) to obtain the HOMA, GEO, and EN indices (Eq. (13)), and the ratio between the HOMA, GEO, and EN values between the benzene rings at the outer and center of the molecule. We note that applying Eq. (11) to estimate the bond length of benzene and naphthalene has resulted in a HOMA

Table 5. The values of HOMA, GEO, and EN of anthracene and phenanthrene from previous studies, and their ratios for the two inequivalent benzene rings.

Anthracene									
HOMA		GEO		EN		HOMA-A/B	GEO-A/B	EN-A/B	Ref.
A	B	A	B	A	B				
0.679	0.797	0.273	0.126	0.049	0.077	0.852	2.167	0.636	[8]
0.619	0.696								[31]
0.629	0.719								[32]
0.742	0.889	0.243	0.068	0.014	0.043	0.835	3.574	0.326	[33]
Phenanthrene									
0.868	0.456	0.076	0.245	0.056	0.296	1.904	0.310	0.189	[3]
0.906	0.552	0.009	0.176	0.085	0.272	1.641	0.051	0.313	[8]
0.856	0.435								[31]
0.868	0.461								[32]
0.918	0.690	0.009	0.069	0.073	0.241	1.330	0.130	0.303	[33]

index of 1.000 and 0.910 for those two molecules, respectively, in good agreement with a previous study.[25] For the HOMA index of anthracene, the results of previous studies show that the benzene ring at the center (B) of anthracene is more aromatic than the outer (A), opposite results to those of phenanthrene.[8,30-33] Table 5 shows the HOMA, GEO, and EN values, as well as their ratios for the two inequivalent benzene rings of anthracene and phenanthrene from previous studies.

Three criteria were used to determine the best values of *a* and γ, namely, the values of the HOMA, GEO, and EN indices; ratio of HOMA, GEO, and EN for the two non-equivalent benzene rings; and standard deviation of the bond length compared to the corresponding values from ref. 33. Figure 4 illustrates the correction results for the

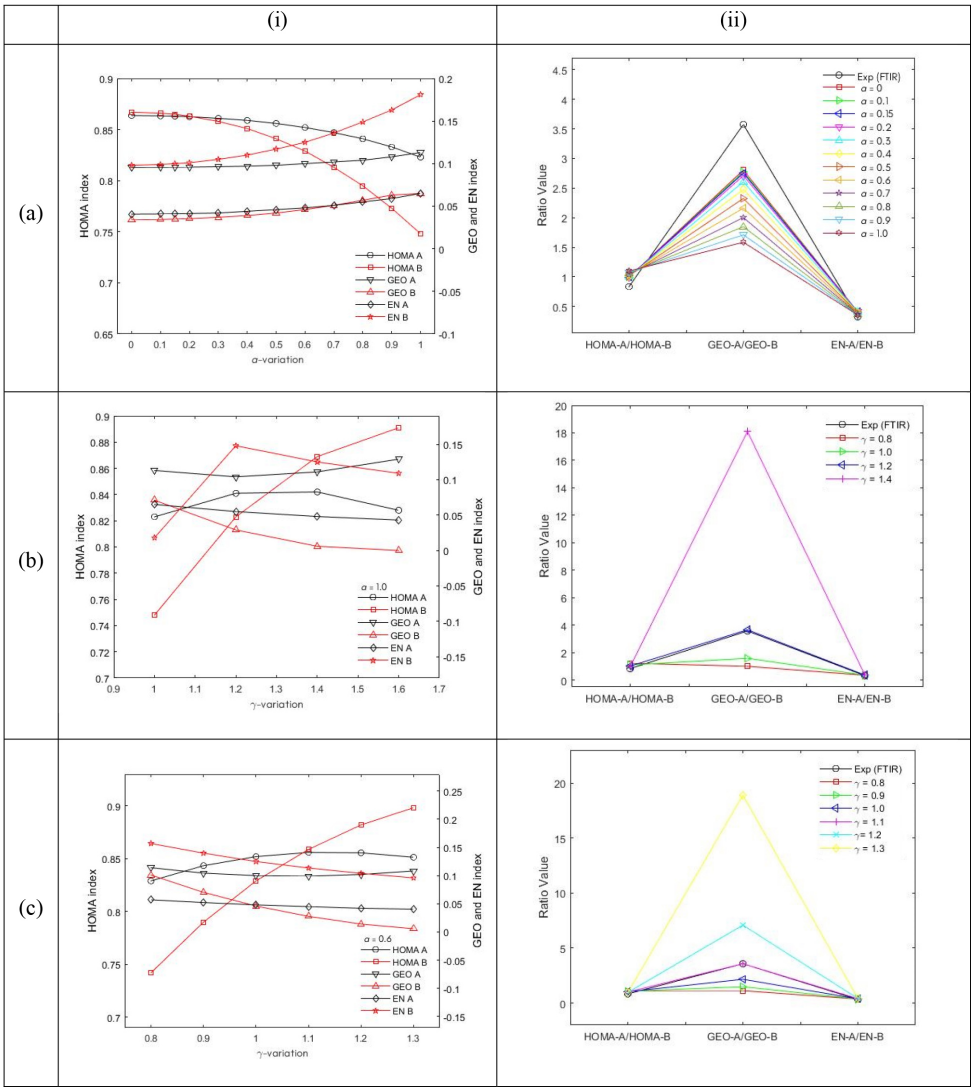

Figure 4. *(i) HOMA, GEO, and EN indices for the outer benzene ring (A) and central benzene ring (B) of the anthracene, and (ii) the ratio of HOMA, GEO, and EN indices of the two benzene rings, for the variation of: (a) Coulomb integral (a) for γ = 1, (b) resonance integral (γ) for a = 1, and (c) resonance integral (γ) for a = 0.6. In figs (ii) the corresponding values from Ref. [33] are also shown for comparison*

Hückel parameter for a variation in the Coulomb integral (α') and resonance integral (β') for the four central carbon atoms of anthracene, expressed in a and γ values. The left figure (i) shows the HOMA, GEO, and EN indices of the outer benzene ring (A) and the central or inner benzene ring (B) of the anthracene; and the right figure (ii) shows the ratio of HOMA, GEO, and EN indices of the two benzene rings, compared with the results of a previous study.[33]

Upon variation of a, we found a non-monotonous variation in the HOMA indices. A qualitative agreement with previous studies, where HOMA-B > HOMA-A was obtained for $a < 0.3$. For γ variation with $a = 1.0$, the condition of HOMA-B > HOMA-A was obtained for $\gamma \geq 1.3$. However, in both cases, the ratio values of HOMA, GEO, and EN for the two non-equivalent benzene rings are relatively far from the values obtained from the experimental results (as most clearly observed for the GEO ratio, except for $a = 1$ and $\gamma = 1.2$). The best result was obtained for $a = 0.6$ and $\gamma = 1.1$ (Figure 4(c)).

Applying the same method to phenanthrene, Figure 5 illustrates the HOMA index and the standard deviation value of bond length upon γ variation for $a = 0.6$. From this figure, HOMA-A > HOMA-B for all γ values. From the three criteria mentioned above, the best result was obtained for $a = 0.6$ and $\gamma = 1.2$, along with the smallest standard deviation value.

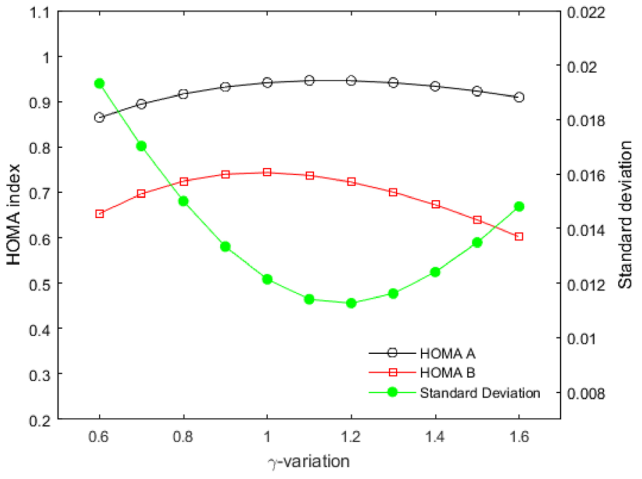

Figure 5. *HOMA indices for the outer benzene ring (A) and central benzene ring (B) of the phenanthrene, along with the standard deviation values of bond length compared to the corresponding values from ref. 33.*

To further validate the result, the calculated bond lengths for some unique bonds of the two molecules for the best parameters, $a = 0.6$ and $\gamma = 1.1$ for anthracene and $a = 0.6$ and $\gamma = 1.2$ for phenanthrene, were compared to previous theoretical and experimental studies, as shown in Figure 6. From this figure, one can see a good agreement for the bond order and bond length pattern with the results of previous studies. For the best results in the correction of the Hückel parameters, the improvement in the standard deviation value of the bond length compared to the original Hückel method was 4.39% for anthracene and 16.71% for phenanthrene.

The molecular energy level diagram for the best result to correct the Hückel parameter and the associated molecular orbital obtained from a linear combination of SALC are shown in Figure 7(a) for anthracene and Figure 7(b) for phenanthrene.

From this figure, the non-degenerate energy levels of anthracene are in good agreement with a previous semi-empirical self-consistent field-linear combination of atomic-molecular orbital study.[9] The lowest energy level corresponds to the delocalization of π electrons, and the number of nodal lines increases with increasing energy level. The HOMO-LUMO gap energy and the delocalization energy of anthracene calculated from this correction were 0.82β and 8.08β, respectively. The corresponding values for phenanthrene were 1.22β and 8.45β. We note that the original Hückel method resulted in HOMO–LUMO gap energy and delocalization energies of 0.82β and 5.31β for anthracene, while for phenanthrene they were 1.22β and 5.45β, respectively. We note that for the two molecules, the HOMO–LUMO gap energy is almost constant both to a and γ variations, while the delocalization energy increases linearly with an increase in a and γ. Thus, the Hückel parameter correction increased the stability of the molecule, as shown by the increase in the delocalization energy.

As also shown in Figure 6, the HOMO–LUMO gap energy and delocalization energy of phenanthrene is larger than that of anthracene. This result is in good agreement with previous quantum mechanical calculation studies based on Hartree Fock,[40] density functional theory,[41] and time-dependent density functional theory methods[41]. The commonly accepted calculated values are 3.23 – 3.64 eV for anthracene[42-44] and 4.02 – 4.74 eV for phenanthrene.[41-42,45] The experimental optical band gap values based on ultraviolet-visible spectroscopy are 3.27 eV for anthracene and 4.16 eV for phenanthrene.[42] Thus, the results presented in this study are in good agreement with previous studies that show that kinked phenanthrene is more stable than straight anthracene.[32,46]

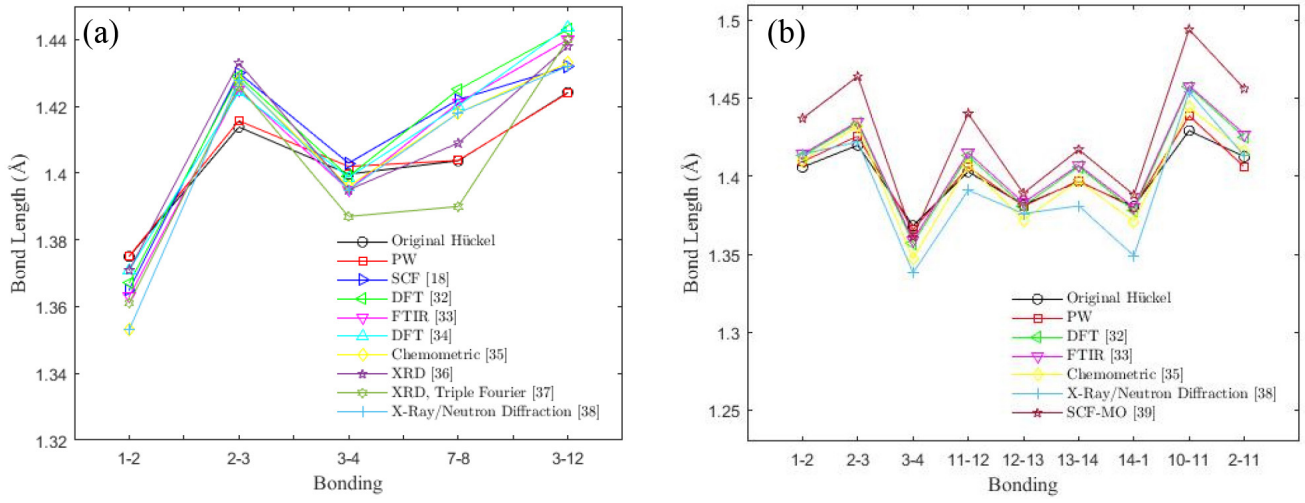

Figure 6. *Bond lengths (a) anthracene and (b) phenanthrene for the best results in the present work compared with the results from original Hückel parameters and previous studies*[18,32-39]

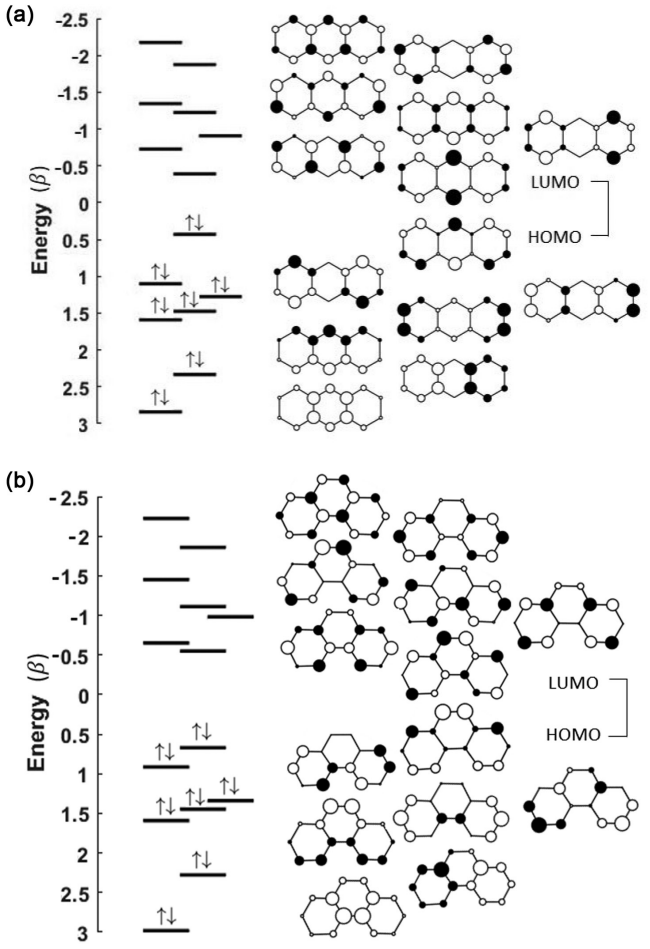

Figure 7. *Molecular energy level diagram of (a) anthracene and (b) phenanthrene for the best result to a correction of Hückel parameters and the associated molecular orbitals. The black and white circles indicate the positive and negative coefficients of SALC, respectively*

CONCLUSIONS

Anthracene with point group D_{2h} shows excessive degeneracy in the energy levels of the π-electron system. Based on the inequivalent carbon atoms and the physical phenomenology of the ring current that flows along the perimeter of the molecule, we proposed a correction to the Hückel parameters. The solution to the Hamiltonian of the π-electron was performed using symmetry group theory to solve the determinant matrix or secular equations in a particular IR. The correction was conducted by introducing a change in the Coulomb energy (α′) for the four central carbon atoms and resonance energy (β′) for C–C bonds along the bridge of the molecule, expressed in terms of a and γ values as a fraction of resonance energy (β). The computational process was performed using MATLAB® software. The resulting linear combination coefficient of the molecular orbital was used to calculate the bond order and bond length, and the results were similar to those of previous studies. The validity of the correction was shown by the values of HOMA, GEO, and EN indices of aromaticity which showed that the central benzene ring is more aromatic than the outer benzene ring. The best result was shown for a = 0.6 and γ = 1.1. Further analysis revealed the non-degenerate energy levels and molecular orbitals obtained as a linear combination of SALCs. We applied the same method to phenanthrene (point group C_{2v}) as the topological analog of anthracene. For this molecule, the outer benzene ring is more aromatic than the central ring, and the best result was shown for a = 0.6 and γ = 1.2. Compared to the original Hückel method, this correction resulted in higher delocalization energy, signifying that the molecule has a higher stability, while the HOMO–LUMO energy gap remains the same. From the HOMO–LUMO energy gap and delocalization energy, phenanthrene is more stable than anthracene, which is in good agreement with previous advanced calculations and experimental studies.

ACKNOWLEDGEMENTS

This study is the output of the P2MI ITB 2022 research scheme. It is dedicated to the late Professor M.O. Tjia for his memorable contributions to conjugated polymers, material physics, and chemistry at the Physics Department, Faculty of Mathematics and Natural Science (FMIPA) of the Institut Teknologi Bandung.

REFERENCES

1. Yates, K.; *Hückel molecular orbital theory*, Academic Press: New York, 2012.
2. Kutzelnigg, W.; *J. Comput. Chem.* **2006**, *28*, 28.
3. Krygowski, T. M.; Szatylowicz, H.; *ChemTexts* **2015**, *1*, 12.
4. Wild, U.; Keller, J.; Gonthard, Hs, H.; *Theor. Chim. Acta* **1969**, *14*, 383-395.
5. Torres, E. M.; *Chem. Educator* **2006**, *16*, 1-8.
6. McQuarrie, D. A.; Simon, J. D.; *Physical chemistry: a molecular approach*, Sterling Publishing Company:New York, 1997.
7. Tjia, M. O.; Sutjahja, I. M.; *Orbital Kuantum (Pengantar Teori dan Contoh Aplikasinya)*, Karya Putra Darwati Bandung: Bandung, 2012.
8. Setiawan, D.; Kraka, E.; Cremer, D.; *J. Org. Chem.* **2016**, *81*, 9669.
9. Fukui, K.; Morokuma, K.; Yonezawa, T.; *Bull. Chem. Soc. Jpn.* **1959**, *32*, 853.
10. Steiner, E.; Fowler, P. W.; *Chem. Commun.* **2001**, 2220.
11. Steiner, E.; Fowler, P. W.; *Int J Quantum Chem* **1996**, *60*, 609.
12. Heine, T.; Islas, R.; Merino,G.; *J. Comput. Chem.* **2006**, *28*, 302.
13. Fowler, P.W.; Steiner, E.; Havenith, R.W.A.; Jenneskens, L.W.; *Magn. Reson. Chem.* **2004**, *42*, S68.
14. Cuesta, I. G.; De Merás, A. S.; Pelloni, S.; Lazzeretti, P.; *J. Comput. Chem.* **2009**, *30*, 551.
15. Steiner, E.; Fowler, P.W.; Havenith, R. W. A.; *J. Phys. Chem. A* **2002**, *106*, 7048.
16. Anusooya, Y.; Chakrabarti, A.; Pati, S. K.; Ramasesha, S.; *Int. J. Quantum Chem.* **1998**, *70*, 503.
17. Stegmann, T.; Villafañe, J. A. F.; Ortiz, Y. P.; Deffner, M.; Herrmann, C.; Kuhl, U.; Mortessagne, F.; Leyvraz, F.; Seligman, T. H.; *Phys. Rev. B* **2020**, *102*, 075405.
18. Pritchard, H. O.; Sumner, F. H.; *Trans. Faraday Soc.* **1955**, *51*, 457.
19. Kruszewski, J.; Krygowski, T. M.; *Tetrahedron Lett.* **1972**, *13*, 3839.
20. Cyrański, M. K.; Krygowski, T. M.; *Tetrahedron*, **1999**, *55*, 6205.
21. Krygowski, T. M.; Cyraliski, M.; *Tetrahedron* **1996**, *52*, 10255.
22. Dobrowolski, J.Cz.; *ACS Omega* **2019**, *4*, 18699.
23. Schleyer, P. von R.; Maerker, C.; Dransfeld, A.; Jiao, H.; van Eikema Hommes, N. J. R.; *J. Am. Chem. Soc.* **1996**, *118*, 6317.
24. Poater, J.; Fradera, X.; Duran, M.; Sola, M.; *Chem. Eur. J.* **2003**, *9*, 400.
25. Kwapisz, J. H.; Stolarczyk, L. Z.; *Struct. Chem.* **2021**, *32*, 1393.
26. Ligabue, A.; Pincelli, U.; Lazzeretti, P.; Zanasi, R.; *J. Am. Chem. Soc.* **1999**, *121*, 5513.
27. Atkins, P.; Friedman, R.; *Molecular Quantum Mechanics*, 4th ed., Oxford University Press: Oxford, 2005.
28. Mataga, N.; Nishimoto, K.; Mataga, S.; *Bull. Chem. Soc. Jpn.* **1959**, *32*, 395.
29. Linus Pauling, *J. Chem. Phys.* **1936**, *4*, 673.
30. Krygowski, T. M.; *J. Chem. Inf. Comput. Sci.* **1993**, *33*, 70.

31. Portella, G.; Poater, J.; Sola, M.; *J. Phys. Org. Chem.* **1993**, *18*, 785.
32. Poater, J.; Duran, M.; Solà M.; *Front. Chem.* **2018**, *6*; 561.
33. Kalescky, R.; Kraka, E.; Cremer, D.; *J. Phys. Chem. A* **2014**, *118*, 223.
34. Fedorov, I. A.; Zhuravlev, Y. N.; Berveno, V. P.; *Phys. Chem. Chem. Phys.* **2011**, *13*, 5679.
35. Kiralj, R.; Ferreira, M. M. C.; *J. Chem. Inf. Comput. Sci.* **2002**, *42*, 508.
36. McL Mathieson, A.; Robertson, J. M.; Sinclair, V. C.; *Acta Cryst.* **1950**, *3*, 245.
37. Sinclair, V. C.; Robertson, J. M.; McL Mathieson, A.; *Acta Cryst*. **1950**, *3*, 251.
38. Kiralj, R.; Kojić-Prodić, B.; Žinić, M.; Alihodžić, S.; Trinajstić, N.; *Acta Cryst.* **1996**, *B52*, 823.
39. Kubba, R. M.; Al-ani, R. I.; Shanshal, M.; *Zeitschrift fur Naturforschung A* **2005**, *60a*, 165.
40. Howard, S. T.; Krygowski, T. M.; *Can. J. Chem.* **1997**, *75*, 1174.
41. Malloci, G.; Cappellini, G.; Mulas, G.; Mattoni, A.; *Chem. Phys.* **2011**, *384*, 19.
42. Menon, A.; Dreyer, J. A. H.; Martin, J. W.; Akroyd, J.; Robertson, J.; Kraft, M.; *Phys. Chem. Chem. Phys.*, **2019**, *21*, 16240.
43. Kukhta, A. V.; Kukhta, I. N.; Kukhta, N. A.; Neyra, O. L.; Meza, E.; *J. Phys. B: At. Mol. Opt. Phys.* **2008**, *41*, 205701.
44. Perger, W. F.; *Chem. Phys. Lett.* **2003**, *368*, 319.
45. Gumuş, A.; Gumuş, S.; *Maced. J. Chem. Chem. Eng.* **2017**, *36,* 243.
46. Poater, J.; Visser, R.; Sola, M.; Bickelhaupt, F. M.; *J. Org. Chem.* **2007**, *72*, 1134.